Electronic Supplementary Information

Membrane-free sequential paired electrosynthesis of 1,4-hydroquinone from phenol over a self-supported electrocatalytic electrode

Wei-Ling Zhang,[abc] Ya-Jing Li,[ab] Yingchun He,[b] Shao Zhang,[b] Haohong Li,[ac] Huidong Zheng*[ac] and Qi-Long Zhu*[bd]*

[a] *College of Chemical Engineering and College of Chemistry, Fuzhou University, Fuzhou 350108, China*

[b] *State Key Laboratory of Structural Chemistry, Fujian Institute of Research on the Structure of Matter, Chinese Academy of Sciences (CAS), Fuzhou 350002, China*

[c] *Qingyuan Innovation Laboratory, Quanzhou 362801, China*

[d] *School of Materials Science and Engineering, Zhejiang Sci-Tech University, Hangzhou 310018, China*

E-mail: zhangshao@fjirsm.ac.cn, youngman@fzu.edu.cn and qlzhu@fjirsm.ac.cn

Materials and reagents

Carbon felt (CF) and graphite (G) were purchased from Tianjin Beihaitansu Co., Ltd. (China). Phenol (≥99%), hydroquinone (≥99%), *p*-benzoquinone (≥99%), catechol (≥99%), *o*-cresol (≥99%), 2,6-dimethylphenol (≥99%), 2,3,5-trimethylphenol (≥98%), 2-chlorophenol (≥99%), 2-fluorophenol (≥98%), methylhydroquinone (≥99%), chlorohydroquinone (≥98%), trimethylhydroquinone (≥98%), 2,6-dimethylhydroquinone (≥98%), 2-fluorobenzene-1,4-diol (≥98%), 1-naphthol (≥99%), 5,6,7,8-tetrahydro-1-naphthol (≥98%) , p-tert-butylphenol (≥98%) were obtained from Aladdin Industrial Co., Ltd. $Pb(NO_3)_2$ (≥99.0%), HNO_3 solution (≥90.0%), H_2SO_4 solution (96%), and NaOH pellet (≥98%), N,N'-dimethylformamide (DMF, ≥99.5%) were bought from Sinopharm Chemical Reagent Co., Ltd. Deuterium oxide (D_2O, 99.9%) was purchased from Shanghai Titan Technology Co., Ltd. The above reagents were used without further purification. Deionized water (≥18.2 MΩ·cm at 25 °C) was used for solution preparation.

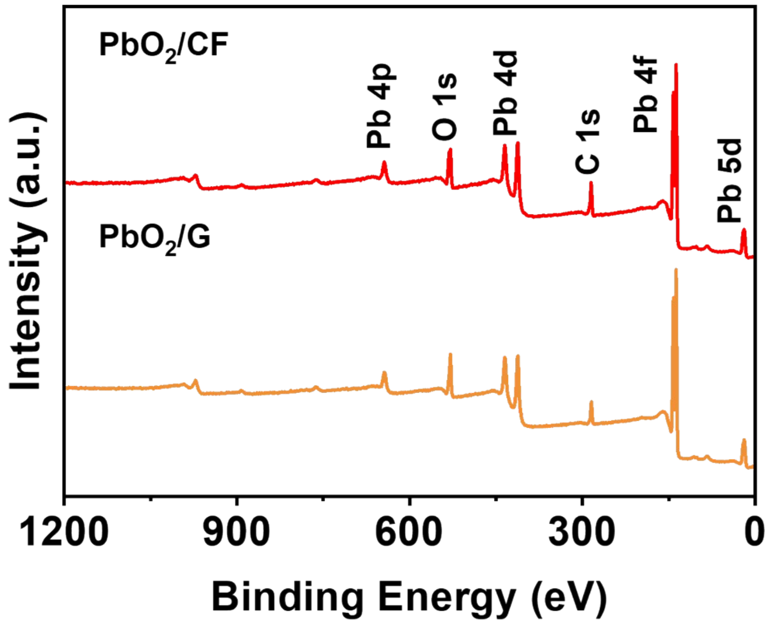

Fig. S1 XPS survey spectra of PbO_2/CF and PbO_2/G.

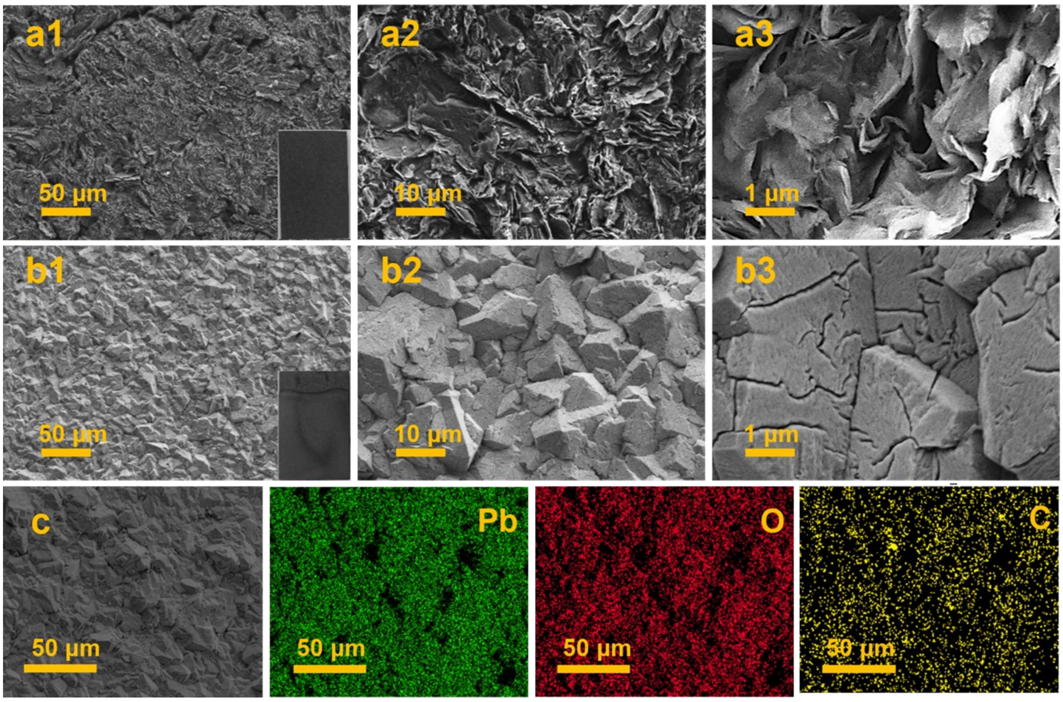

Fig. S2 SEM images of (a1-a3) bare graphite substrate and (b1-b3) PbO_2/G; (c) EDX elemental mapping images of PbO_2/G.

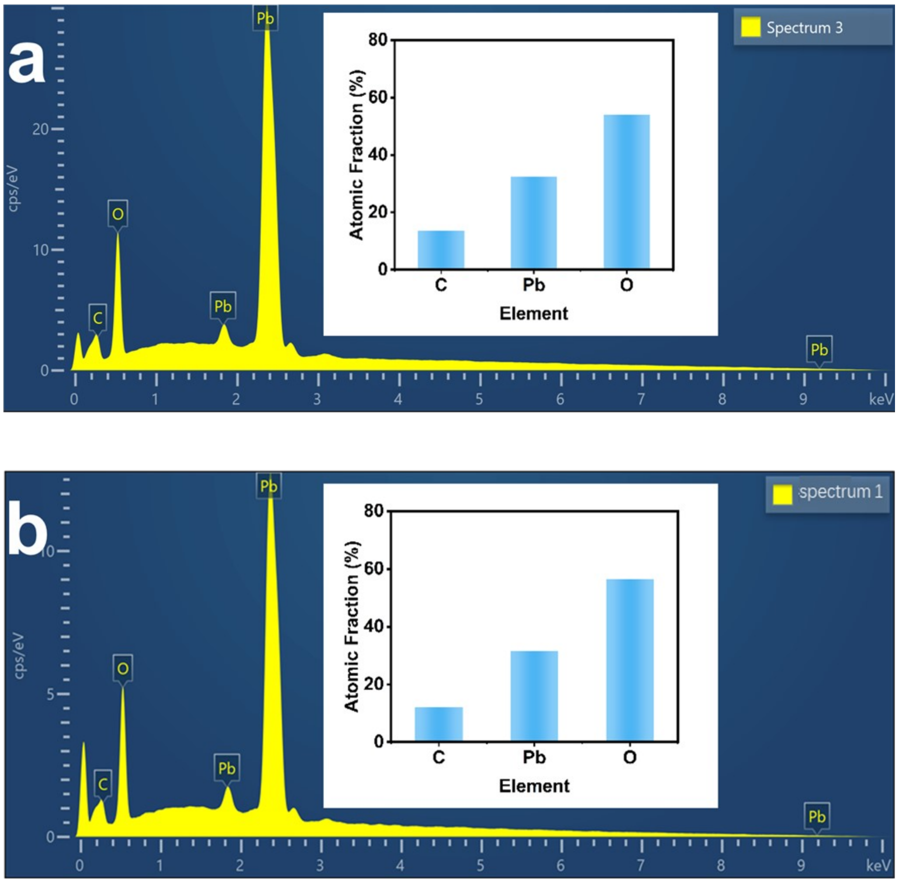

Fig. S3 EDX elemental analysis of (a) PbO_2/CF and (b) PbO_2/G.

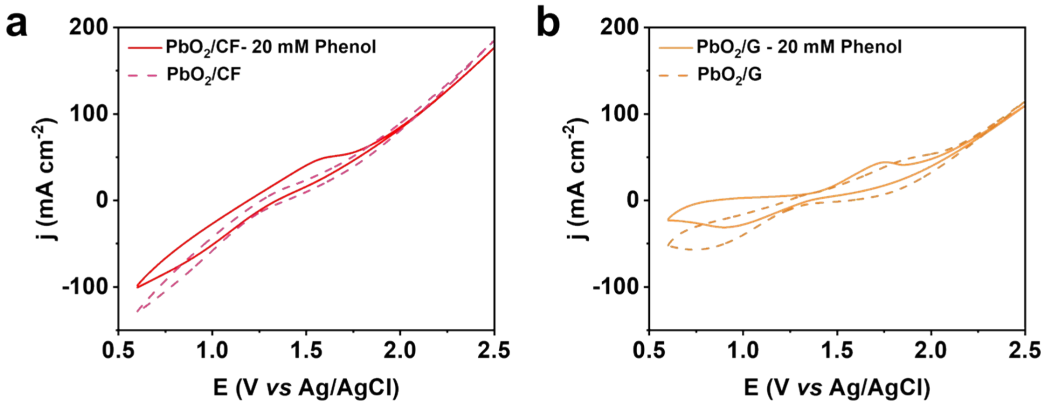

Fig. S4 CV curves at the scan rate of 100 mV s^{-1} in 0.1 M H_2SO_4 with and without 20 mM phenol over (a) PbO_2/CF and (b) PbO_2/G.

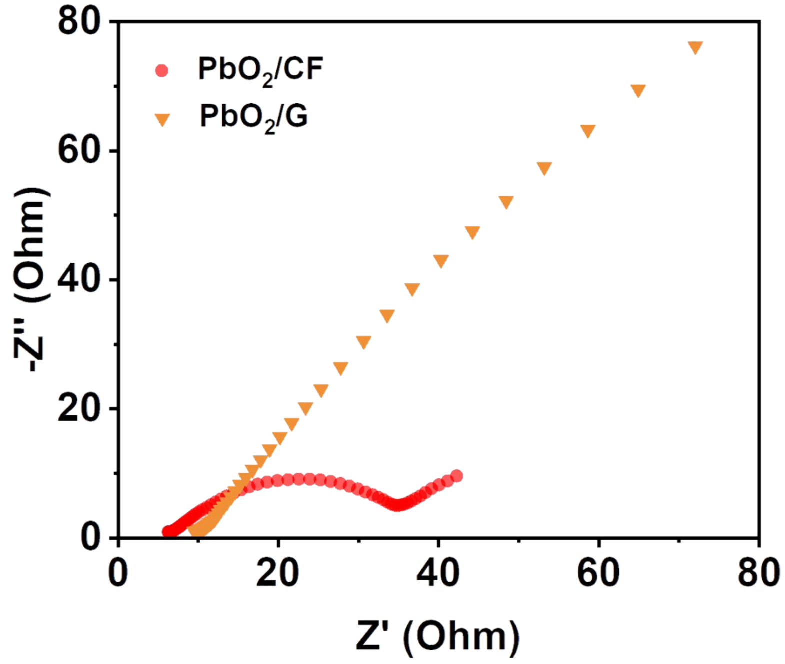

Fig. S5 EIS Nyquist plots in 0.1 M H_2SO_4 with 20 mM phenol.

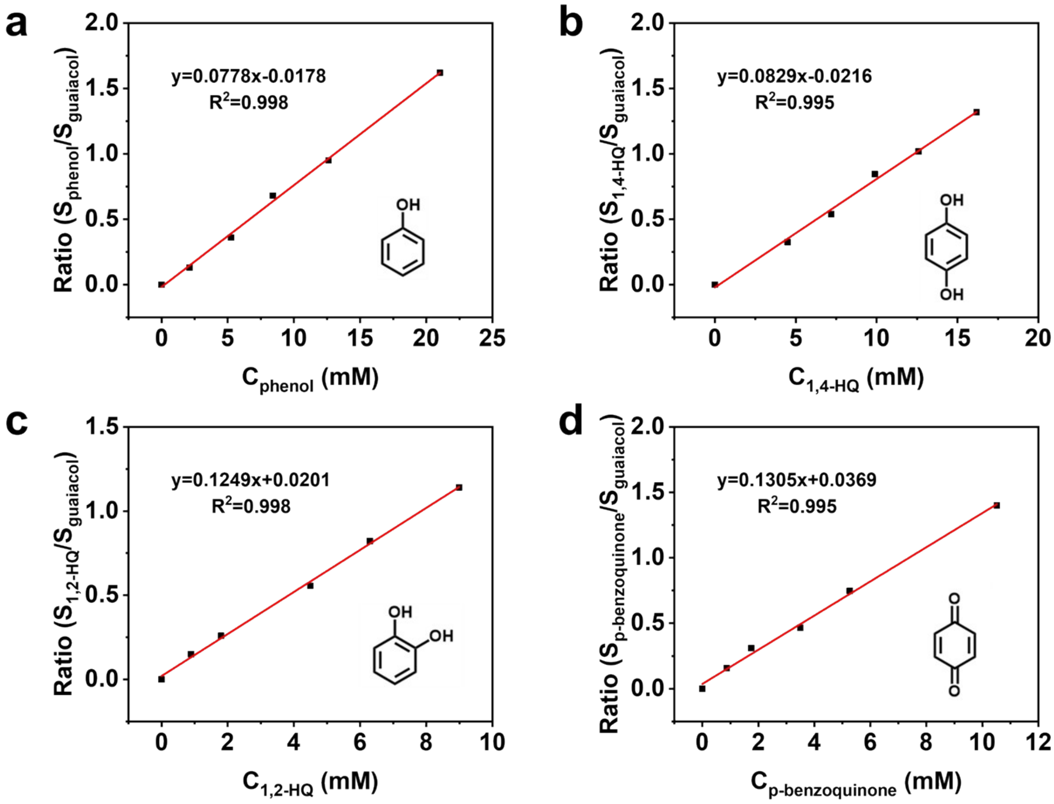

Fig. S6 The calibration curves used to quantify the concentration of phenol, 1,4-HQ, 1,2-HQ, and p-benzoquinone in the electrolyte.

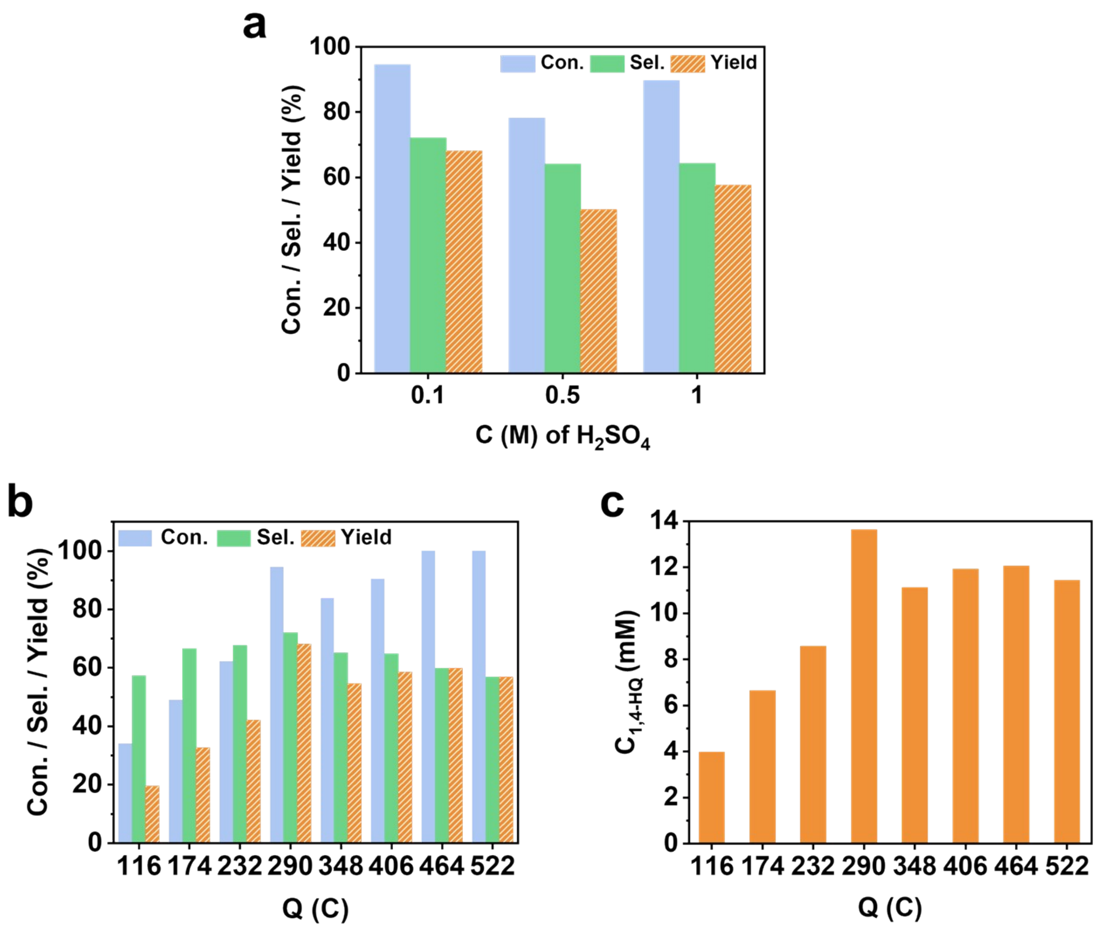

Fig. S7 Phenol conversions, 1,4-HQ selectivity and yields over PbO_2/CF (a) in a quantified concentration of H_2SO_4 aqueous solution (1, 0.5, 0.1 M) with an applied charge of 290 C at 10 mA cm^{-2}; or (b) against the amount of applied charge in 0.1 M H_2SO_4 at 10 mA cm^{-2}; (c) the concentration of 1,4-HQ against the amount of applied charge.

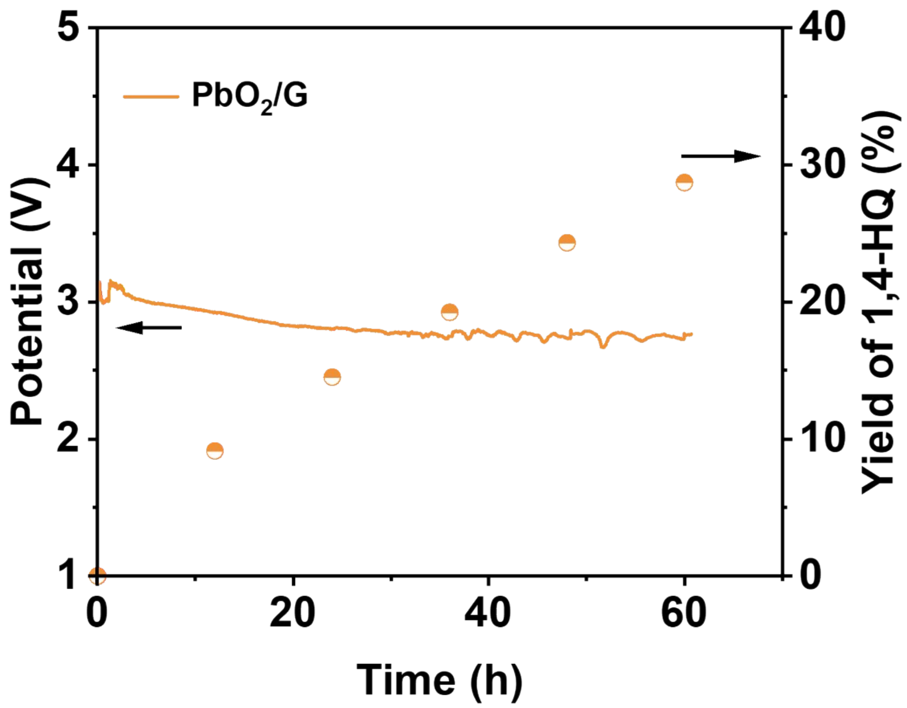

Fig. S8 Galvanostatic test of PbO_2/G with 45 mM phenol in 0.1 M H_2SO_4 solution (75 mL) at 10 mA cm^{-2}.

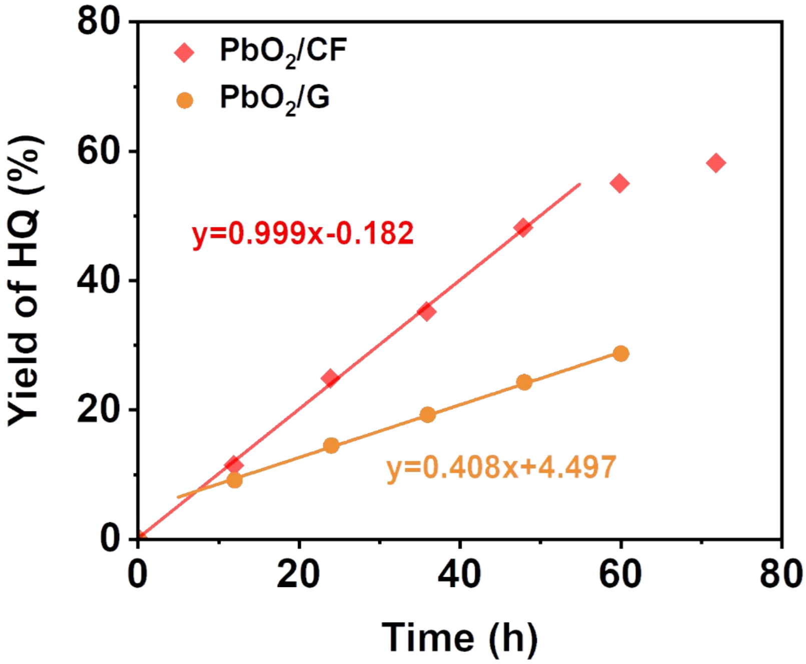

Fig. S9 The corresponding kinetic analysis of galvanostatic test of PbO_2/CF and PbO_2/G with 45 mM phenol in 0.1 M H_2SO_4 solution (75 mL) at 10 mA cm^{-2}.

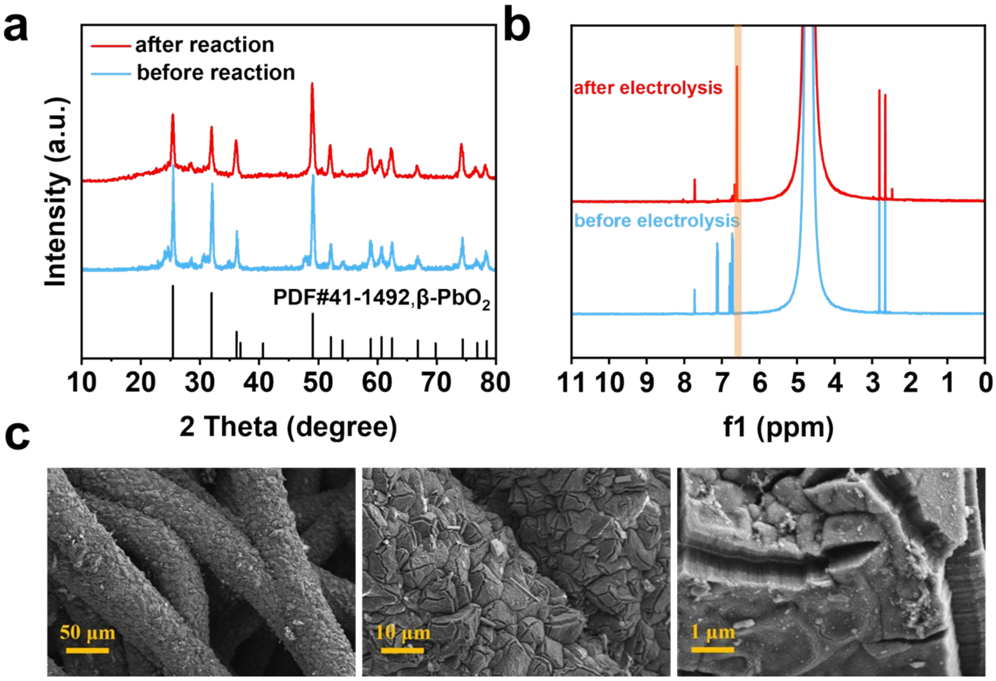

Fig. S10 (a) XRD pattern (b) [1]H NMR spectra and (c) SEM images of PbO_2/CF after long-term electrolysis test for 144 hours.

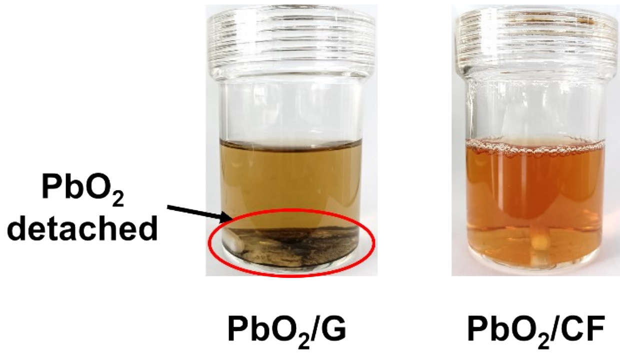

Fig. S11 The optical photographs of electrolyte solution after electrolysis on PbO_2/G (left) and PbO_2/CF (right).

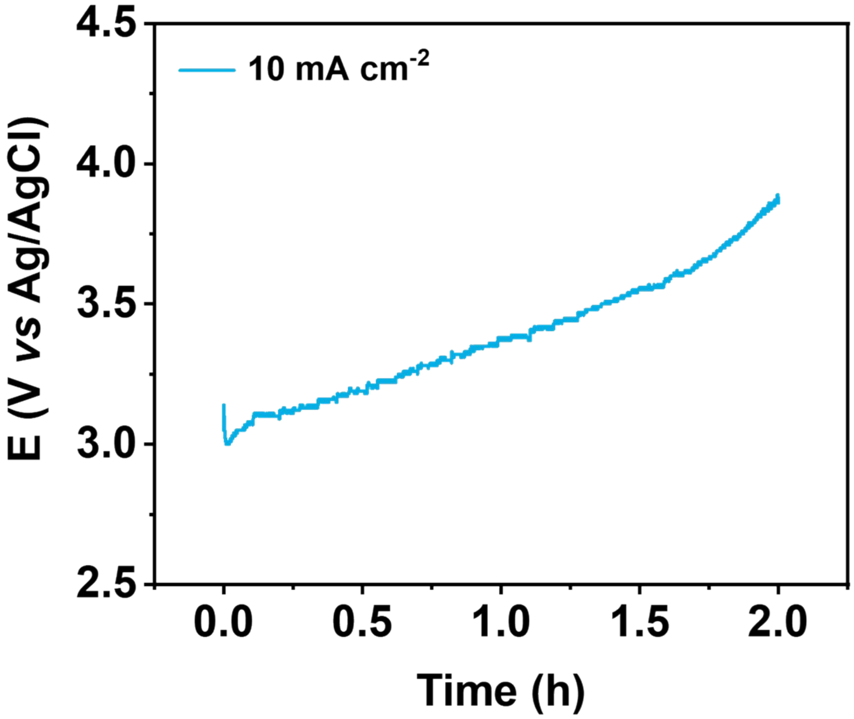

Fig. S12 The anode potential for phenol oxidation by CF substrate in 30 mL of 0.1 M H_2SO_4 with 20 mM phenol.

The utilization of CF as the anode electrode was observed to result in poor stability, possibly due to excessive adsorption of the organic compounds on the electrode surface and subsequent reduction of its conductivity.

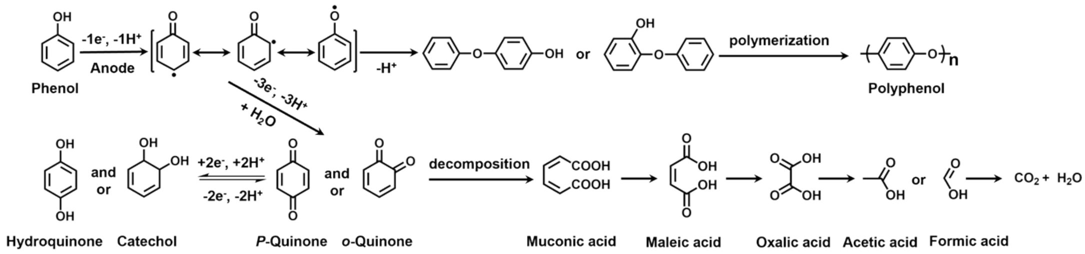

Scheme S1 The possible reaction pathways involved during the electrolysis of phenol.

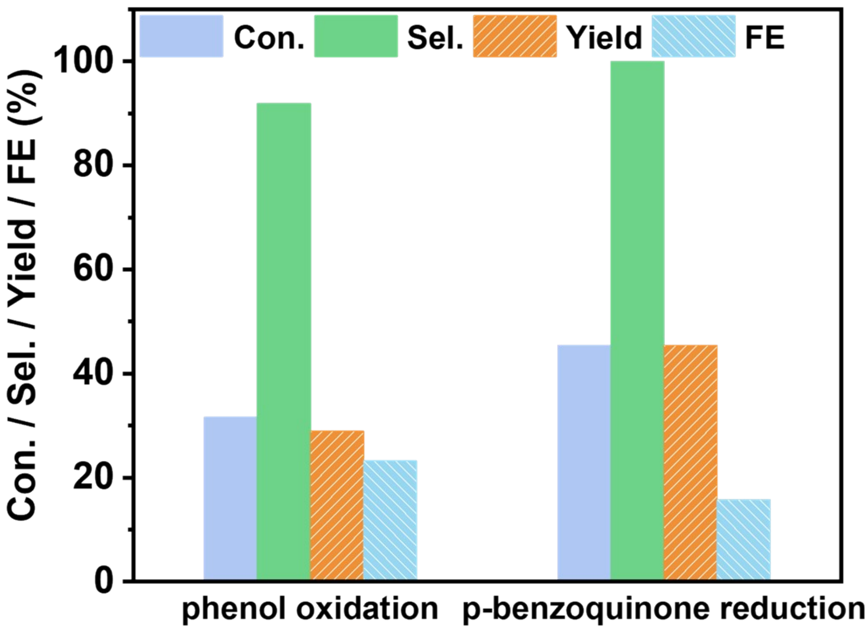

Fig. S13 The electrocatalysis in a divided cell for phenol oxidation and p-benzoquinone reduction over PbO_2/CF.

The reaction conditions: 30 mL of 0.1 M H_2SO_4 with 20 mM phenol and 30 mL of 0.1 M H_2SO_4 with 20 mM p-benzoquinone as the electrolyte, respectively; constant current of 10 mA cm^{-2} at room temperature; applied charges of 290 C; PbO_2/CF electrode and carbon cloth were used as the anode and cathode, respectively. The products were determined by GC analysis.

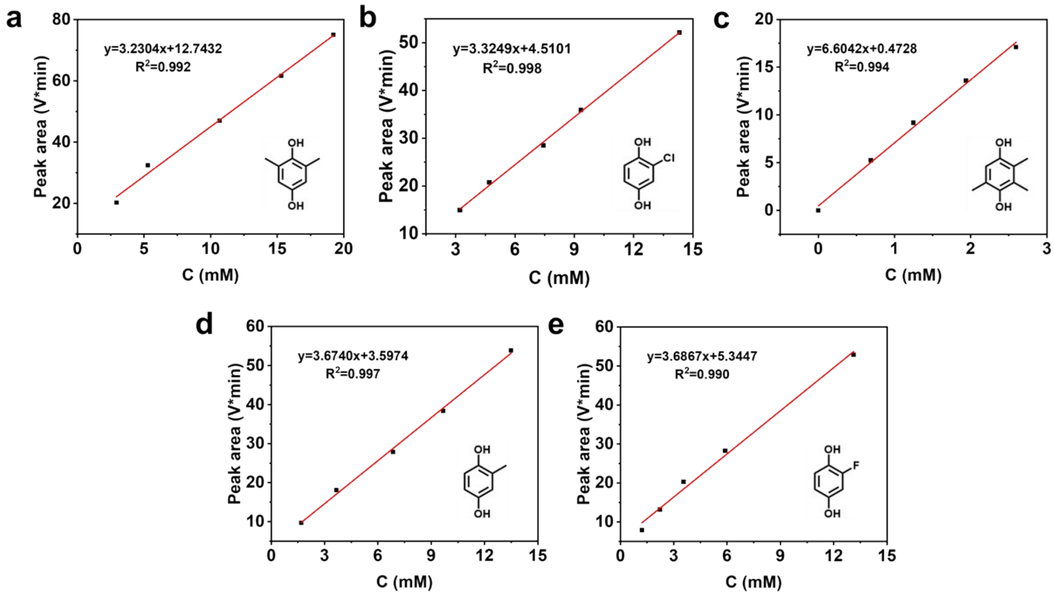

Fig. S14 The calibration curves for products from various reaction substrates.

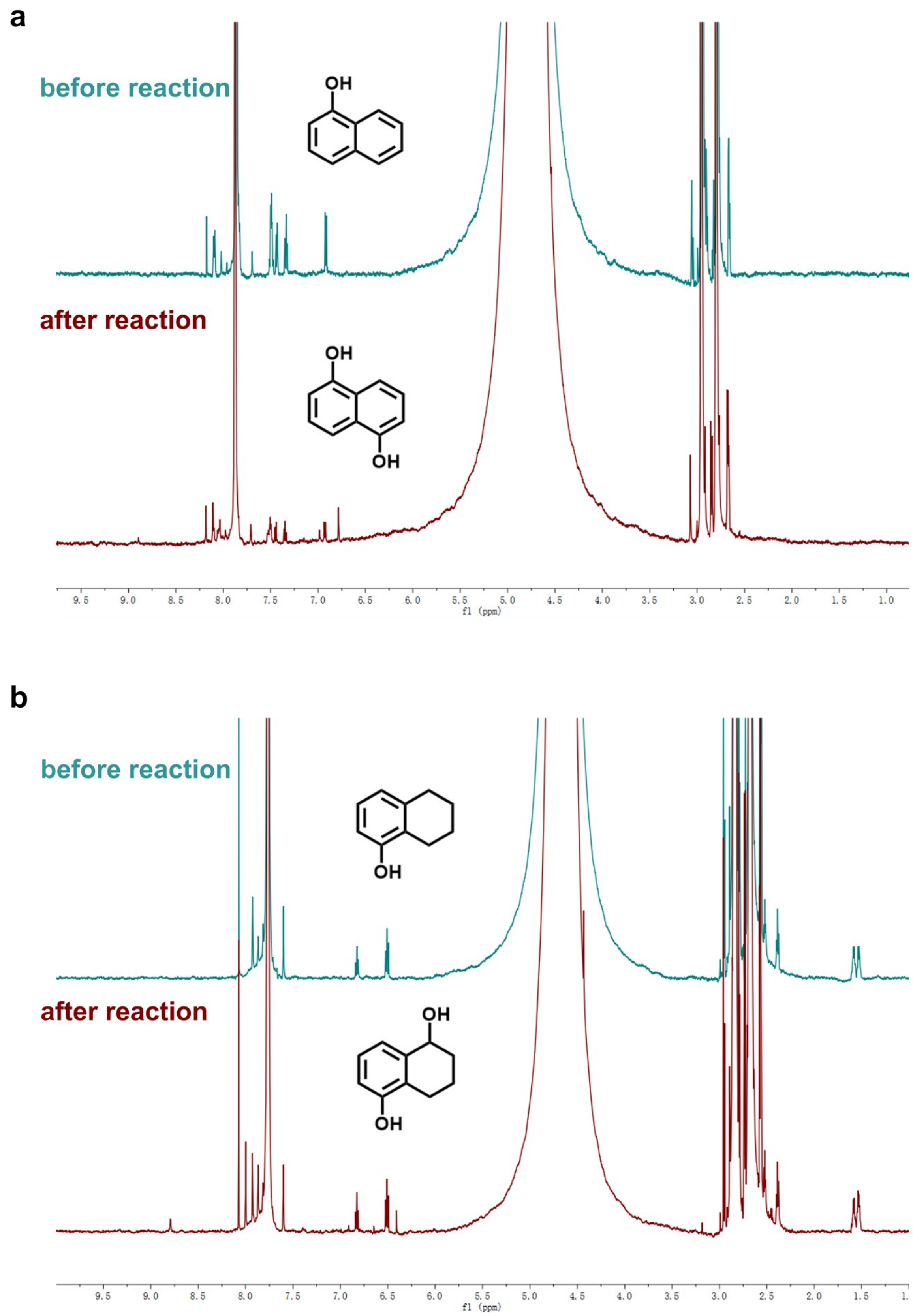

Fig. S15 The [1]H NMR spectra of (a) 1-naphthol and (b) 5,6,7,8-tetrahydro-1-naphthol before and after the electrocatalytic reactions.

The reaction conditions: 30 mL of 0.1 M H_2SO_4 with 20 mM 1-naphthol and 30 mL of 0.1 M H_2SO_4 with 20 mM 5,6,7,8-tetrahydro-1-naphthol as the electrolyte, respectively; constant current of 10 mA cm^{-2} at room temperature; applied charges of 290 C; PbO_2/CF electrode and carbon cloth were used as the anode and cathode, respectively. The products were determined by ^1H NMR.

In the further extension of substrate scope, 1-naphthol and 5,6,7,8-tetrahydro-1-naphthol were selected as the substrates and the experiments were performed in a 0.1 M sulfuric acid aqueous solution at 10 mA cm^{-2}. The solution was tested by ^1H NMR before and after the reaction. As shown in the figures above, the products obtained after the reaction mainly contain the corresponding para-substituted phenols.

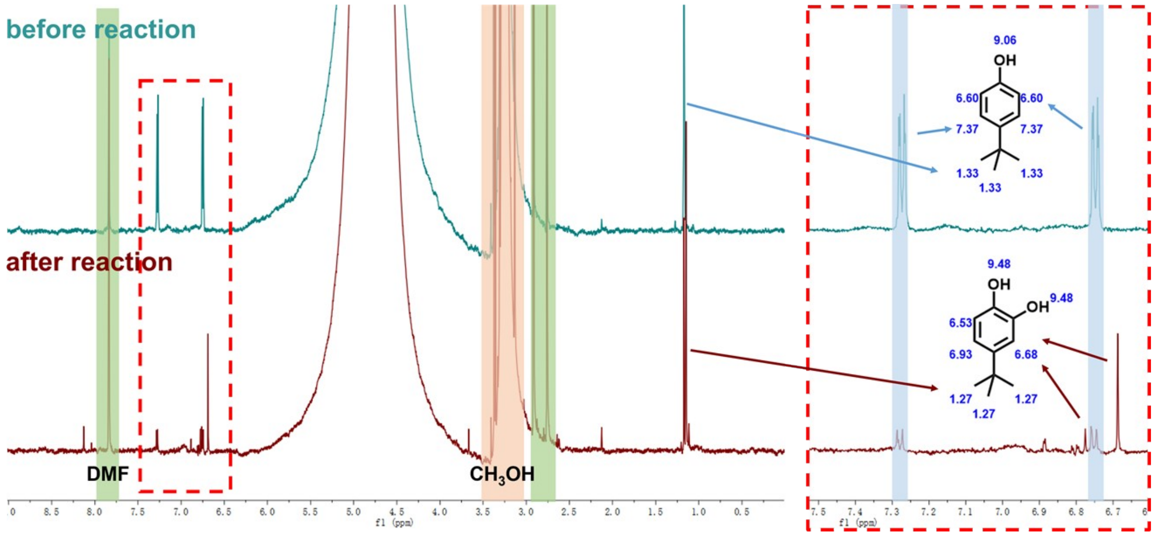

Fig. S16 The [1]H NMR spectra of p-tert-butylphenol before and after the electrocatalytic reaction.

The reaction conditions: 30 mL of 0.1 M H_2SO_4 with 20 mM p-tert-butylphenol as the electrolyte; constant current of 10 mA cm^{-2} at room temperature; applied charges of 290 C; PbO_2/CF electrode and carbon cloth were used as the anode and cathode, respectively. The products were determined by ^1H NMR.

We chose p-tert-butylphenol as a p-substituted phenol substrate. The ^1H NMR results of the substrate before and after electrolysis in 0.1 M H_2SO_4 were compared, which demonstrated that the main product is p-tert-butylcatechol. This result indicates that 1, 2-hydroquinone will be produced when the p-substituted phenol is used as the reactant.

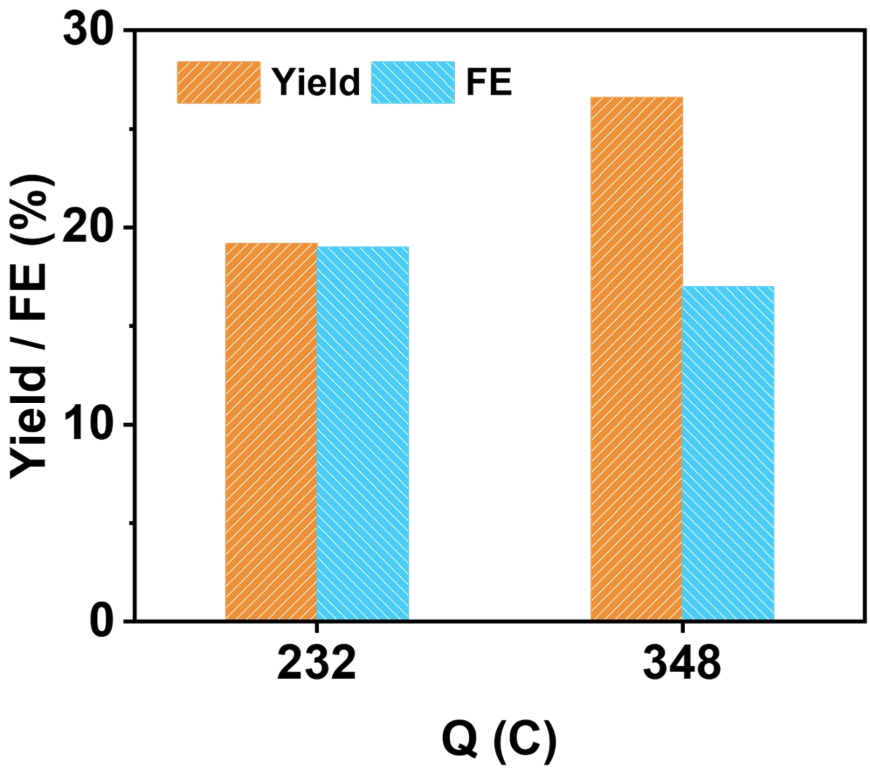

Fig. S17 The yield and Faradaic efficiency of 1,4-HQ in a continuously flowing electrolyzer.

The reaction conditions: 30 mL of 0.1 M H_2SO_4 with 20 mM phenol as the electrolyte; constant current of 10 mA cm^{-2} at room temperature; PbO_2/CF electrode and carbon cloth were used as the anode and cathode, respectively.

A continuously flowing electrolyzer was used to evaluate the electrocatalytic performance of PbO_2/CF for the conversion of phenol. However, the reaction performance was not satisfactory. The efficiency and yield of the electrolysis were found to be below the levels obtained in the undivided cell.

Table S1 Comparison of the performance for 1,4-HQ synthesis with different methods.

Catalysts	Reaction conditions	Oxidation agent	Solvent	Phenol conversion	Product selectivity	Ref.
PbO_2/CF	10 mA cm^{-2}	H_2O	0.1 M H_2SO_4	94.5%	72.1% (1,4-HQ)	This work
NiFe-NS	Xe lamp 550 nm	H_2O_2	H_2O	39.7%	30.0% (1,4-HQ) 69.0% (CAT)	1
Fe-Al-MFI	UV	H_2O_2	H_2O and CH_3CN	80.0%	42.8% (1,4-HQ) 57.1% (CAT)	2
Fe-Al-silicate	UV	H_2O_2	H_2O and CH_3CN	64.9%	34.4% (1,4-HQ) 60.6% (CAT)	3
FTS-50-D	65 °C	H_2O_2	H_2O	45.2%	51.1% (1,4-HQ) 44.1% (CAT)	4
Cu-TS-1	80 °C	H_2O_2	Acetone	49.7%	51.0% (1,4-HQ) 48.2% (CAT)	5
Fe-HMS	40 °C	H_2O_2	H_2O	25.7%	71.5% (1,4-HQ) 24.6% (CAT)	6
CuMgAl-LDH@mSiO_2	65 °C	H_2O_2	H_2O	45.6%	36.6% (1,4-HQ) 60.7% (CAT)	7
POV	25 °C	H_2O_2	H_2O	55.4%	49.6% (1,4-HQ) 50.3% (CAT)	8

CAT: catechol; 1,4-HQ: 1,4-hydroquinone.

References

1 J. Wang, Y. Xu, J. Li, X. Ma, S. Xu, R. Gao, Y. Zhao and Y. Song, Highly selective photo-hydroxylation of phenol using ultrathin NiFe-layered double hydroxide nanosheets under visible-light up to 550 nm, *Green Chem*., 2020, **22**, 8604-8613.

2 A. Kessouri, B. Boukoussa, A. Bengueddach and R. Hamacha, Synthesis of iron-MFI zeolite and its photocatalytic application for hydroxylation of phenol, *Res. Chem. Intermed*., 2018, **44**, 2475–2487.

3 H. Shi, T. Zhang, B. Li, X. Wang, M. He and M. Qiu, Photocatalytic hydroxylation of phenol with Fe–Al-silicate photocatalyst: A clean and highly selective synthesis of dihydroxybenzenes, *Catal. Commun*., 2011, **12**, 1022–1026.

4 H. Li, Y. Zhai, X. Zhang, G. Lv, Y. Shen, X. Wang, T. Jiang and Y. Wu, Iron-containing TS-1 zeolites with controllable mesopores by desilication and their application in phenol hydroxylation, *Ind. Eng. Chem. Res*., 2020, **59**, 10289–10297.

5 G. Wu, J. Xiao, L. Zhang, W. Wang, Y. Hong, H. Huang, Y. Jiang, L. Li and C. Wang, Copper-modified TS-1 catalyzed hydroxylation of phenol with hydrogen peroxide as the oxidant, *RSC Adv*., 2016, **6**, 101071–101078.

6 K. Chellal, K. Bachari and F. Sadi, Catalytic properties of Fe-HMS materials in the phenol oxidation, *Kinet. Catal*., 2014, **55**, 467–473.

7 G. Cui, F. Wang, S. He and M. Wei, Catalytic performance of layered double hydroxide nanosheets toward phenol hydroxylation, *RSC Adv*., 2016, **6**, 105406–105411.

8 I.M. Walton, J.M. Cox, C.A. Benson, D. (Dan) G. Patel, Y.-S. Chen and J.B. Benedict, The role of atropisomers on the photo-reactivity and fatigue of diarylethene-based metal–organic frameworks, *New J. Chem*., 2016, **40**, 101–106.